

# Pitch-Dependent Acceleration of Neurite Outgrowth on Nanostructured Anodized Aluminum Oxide Substrates\*\*

Woo Kyung Cho, Kyungtae Kang, Gyumin Kang, Min Jee Jang, Yoonkey Nam,\* and Insung S. Choi\*

Nervous systems are composed of microstructured scaffolds with three-dimensional nanofeatured textures. These textures enable the systems to give nanometer-scaled physical cues to the overlying cells, along with biochemical cues. However, the topographical effects on the neurons are still an unexplored territory, although there have been many reports on the biochemical cues for neuronal behavior.<sup>[1]</sup> It is practically very difficult to investigate the topographical environments in vivo in the biological systems and/or to mimic them precisely in vitro. There is much recent evidence that the cellular response is affected by the physical properties of artificial materials.<sup>[2]</sup> Studies with such materials could therefore provide us with new insight into the developmental processes of the brain and enable elucidation of the unexplored nanotopographical effects on neuronal behavior.

The responses of nerve cells to surface roughness have been studied on various substrates, such as porous silicon,<sup>[3]</sup> thin titanium nitride films,<sup>[4]</sup> carbon nanotubes,<sup>[5]</sup> topographically molded poly(dimethylsiloxane),<sup>[6,7]</sup> silicon pillar arrays,<sup>[8]</sup> gallium phosphide nanowires,<sup>[9]</sup> aligned nanofiber arrays,<sup>[10]</sup> and silicon nanowires.<sup>[11]</sup> Previous studies showed that nerve cells exhibit enhanced attachment and viability<sup>[3–6]</sup> as well as the axonal guidance effect<sup>[7–10,12,13]</sup> on rough surfaces, as opposed to topographically flat surfaces. However, there have been few reports on how nanometer-scaled

features regulate neuronal behavior in terms of neurite development.

To generate nanotopographical stimuli to neurons in a controllable and systematic manner, it is necessary to make reproducible, rigid structures with variable topographical features. Among the methods for creating topographies on surfaces at the nanometer scale, the fabrication of anodized aluminum oxide (AAO) is highly effective, straightforward,

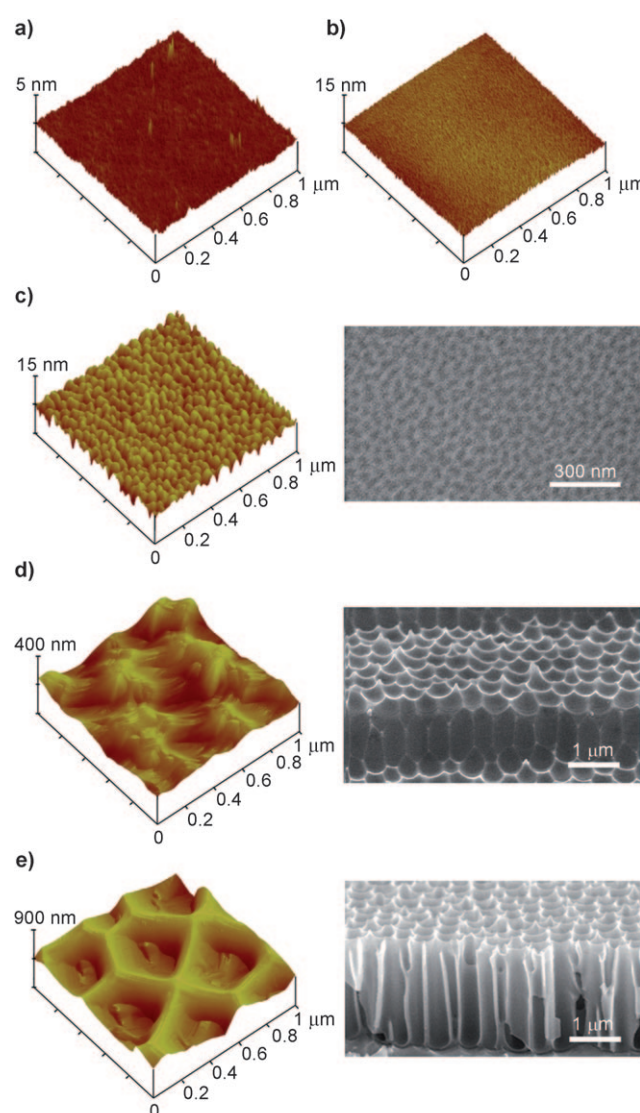


**Figure 1.** Surface topography of the prepared substrates: a) glass and b) flat substrates (AFM images); c) small-concave, d) large-concave, and e) nanoporous substrates (AFM and FE-SEM images).

[\*] Dr. W. K. Cho, K. Kang, Prof. Dr. I. S. Choi  
Molecular-Level Interface Research Center  
Department of Chemistry, KAIST  
Daejeon 305-701 (Korea)  
Fax: (+82) 42-350-2810  
E-mail: ischoi@kaist.ac.kr  
Homepage: <http://cisgroup.kaist.ac.kr>

Prof. Dr. I. S. Choi  
Department of Bio and Brain Engineering, KAIST  
Daejeon 305-701 (Korea)

G. Kang, M. J. Jang, Prof. Dr. Y. Nam  
Department of Bio and Brain Engineering, KAIST  
Daejeon 305-701 (Korea)  
Fax: (+82) 42-350-4310  
E-mail: ynam@kaist.ac.kr  
Homepage: <http://neuros.kaist.ac.kr>

[\*\*] This research was supported through the Basic Science Research Programs by the National Research Foundation of Korea (NRF), funded by the Ministry of Education, Science and Technology (2010-0001953, 2009-0080081, and 2010-0000419), and by the Brain Research Center of the 21st Century Frontier Research Program. I.S.C. thanks the LG Yonam Foundation.

Supporting information for this article is available on the WWW under <http://dx.doi.org/10.1002/ange.201003307>.

inexpensive, and reproducible. AAO nanostructures can be prepared by electrochemically anodizing pure aluminum plates, and their structural features can be varied readily and reproducibly by controlling the experimental parameters.<sup>[14]</sup> Furthermore, the approach can be applied to large-scale areas. Recently, we fabricated AAO nanostructures with diverse degrees of roughness and used them as a model system for water-repellent surfaces.<sup>[15]</sup> We also utilized nanoporous AAO templates to make a gecko-mimetic “hairy” nanopillar system.<sup>[16]</sup> Nanoporous AAO substrates have also been used as a cellular interface for primary human osteoblast-like cells<sup>[17]</sup> and nerve cells,<sup>[18]</sup> and have been embedded in a silicon-based microfluidic system to generate a drug-testing platform.<sup>[19]</sup> In this study, we fabricated four different types of AAO-based nanotopographical substrates, and investigated how various AAO nanostructures affected the development of primary hippocampal neurons. In particular, we focused on neurite development during the first two days: cultured neurons were categorized into three developmental stages, and their growth was analyzed by neurite-length measurement. We also carried out field emission scanning electron microscopy (FE-SEM) studies to investigate the neurite responses to various surface topographies.

The four different substrates were named flat, small concave, large concave, and nanoporous (Figure 1). A glass substrate (coverslip), which had a flat topography and which has been widely used as a substrate<sup>[20]</sup> for the culture of nerve cells, was used as a control. Flat and small-concave AAO substrates were fabricated by the controlled electropolishing of aluminum sheets. The surface structure of the small-concave substrate was characterized as being composed of hexagon-like arrangements of hemispherical concave features (Figure 1c). The pitch between small concave features was about 60 nm. Figure 1d shows typical AFM and cross-sectional FE-SEM images of the textured large-concave substrate that was formed by anodizing the small-concave sheet in 0.9 M  $\text{H}_3\text{PO}_4$  solution and subsequently removing the  $\text{Al}_2\text{O}_3$  layer. The pitch of the large-concave substrate was about 400–450 nm. Further anodization of the large-concave substrate produced the nanoporous substrate with cylindrical pore channels at the center of large concave features (Figure 1e). The four substrates were additionally classified as short-pitch substrates (flat and small concave) and long-pitch substrates (large concave and nanoporous).

To explore neurite outgrowth on various nanotopographies, we cultured primary hippocampal neurons on the *N*-(2-aminoethyl)-3-aminopropyltrimethoxysilane-coated sub-

strates with a seeding density of  $50 \text{ cells mm}^{-2}$  (see the Supporting Information for the results of neuron culture on bare AAO substrates). Figure 2a,b shows fluorescence micrographs of the cells cultured on these substrates after 1 and 2 days of cultivation. In the flat and small-concave substrates (group 1), neurons were surrounded by flattened lamellipodia

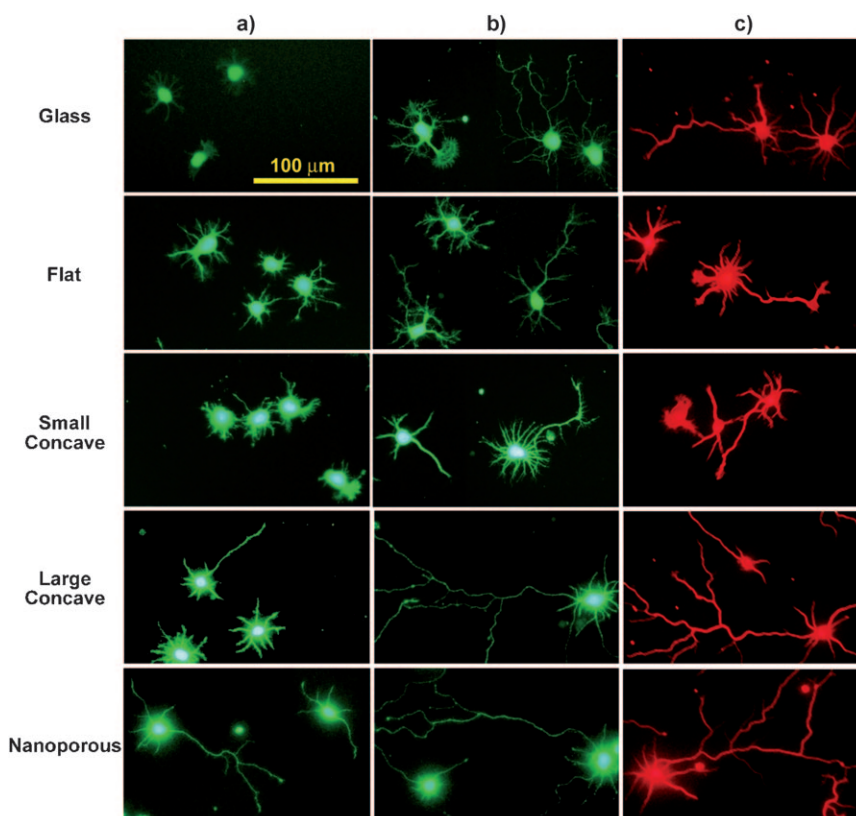


**Figure 2.** Fluorescence micrographs of hippocampal neurons cultured on topographically different substrates. a,b) Cell morphology at 1 DIV (a) and 2 DIV (b); staining with calcein acetoxymethyl ester. c) Immunostaining of class III  $\beta$ -tubulin at 2 DIV.

or showed only short neurites at 1 day in vitro (DIV). At 2 DIV, a major neurite, which would become an axon, started to emerge from the soma of some neurons, and others remained with short neurites. In contrast, in the large-concave and nanoporous substrates (group 2), neurons with major neurites were observed in the culture at 1 DIV. Considering the known developmental processes of hippocampal neurons cultured on a coverslip (major neurites typically stretched out from the soma after 1.5 DIV<sup>[21]</sup>), the observed early neurite outgrowth and extension in group 2 was significant. At 2 DIV, the outgrowth of major neurites from neurons in group 2 became more discernible, and their lengths became longer than at 1 DIV. These intriguing results from group 2 implied that nanoscaled surface pitches had a strong influence on neuronal development. Figure 2c shows the immunostaining of class III  $\beta$ -tubulin, which appeared to be uniformly distributed throughout the cells. The uniform distribution of microtubules indicates the occurrence of neurite developmental processes throughout the entire cell.

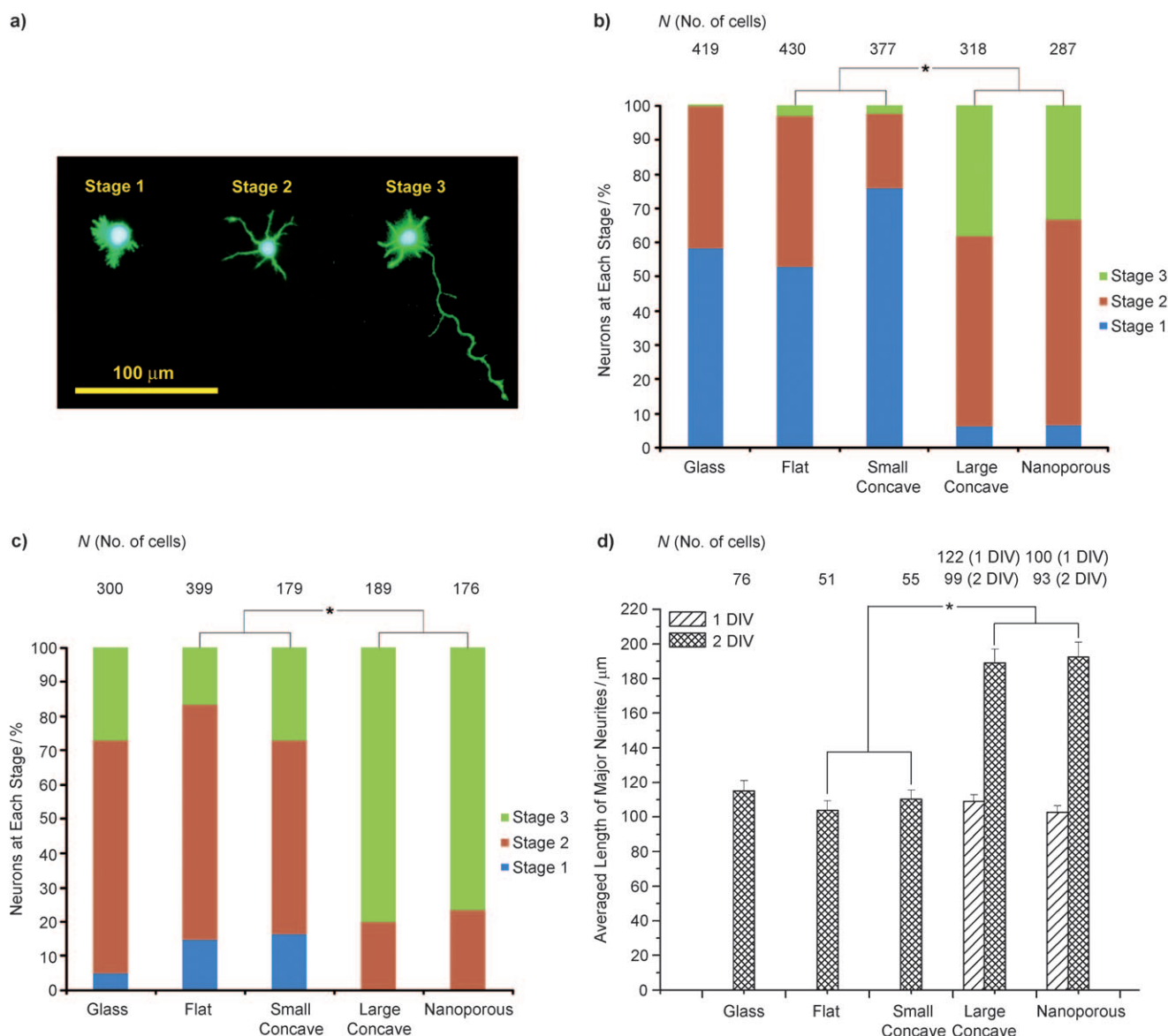


**Figure 3.** a) Classified developmental stages of neurons. b,c) Percentage of neurons at each stage at 1 DIV (b) and 2 DIV (c) for neurons grown on topographically different substrates. The results from group 1 and group 2 were compared with the chi-square test. There was a significant difference between the two groups ( $*p < 0.001$ ). d) Average lengths ( $\pm$  standard error) of major neurites grown on various substrates. All results at 2 DIV were compared by a Student *t* test at the significant level of 99%. There was apparent statistical significance between the two groups ( $*p < 0.001$ ). The numbers of counted cells for the analysis are shown above the graph.

To analyze and study the nanotopographical effect on neurite outgrowth in detail, we focused on neurite development during the first two days. The cultured neurons were classified into three developmental stages by using a previously reported criterion (Figure 3a):<sup>[21]</sup> After neurons attach to substrates, they extend lamellipodia all around the cell body (stage 1). The lamellipodia then coalesce at several discrete sites around the cell periphery, where short neurites begin to extend with growth cones at their ends (stage 2). At this stage, neurites extend and retract over short distances, but there is scarcely any net growth, and the cell retains its symmetrical appearance. At stage 3, one neurite (major neurite) grows for an extended period of time without

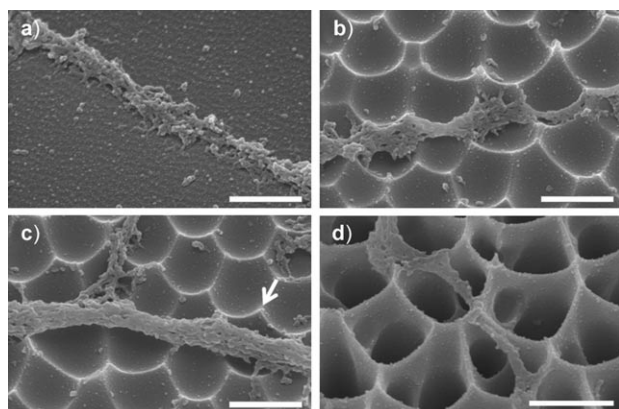
retracting, until it is two or three times longer than the other neurites, to become an axon, and the morphology of the cell becomes polarized.

Figure 3b,c shows the percentage of counted neurons in each categorized stage for neurons grown on topographically different substrates. In group 1, more than 50% of the cells were at stage 1 at 1 DIV, whereas in group 2, 30–35% of the cells had already evolved to stage 3, and only 7% were at stage 1 (Figure 3b). At 2 DIV, a few cells in group 1 were at stage 3, but the percentage of cells was still lower than that observed for group 2 at 1 DIV (Figure 3c). According to the statistical analysis, the ratio of the developmental stages was significantly different between group 1 and group 2; thus, the



pitch, whether short or long, had an effect on the growth of hippocampal neurons. Figure 3d shows the measured average lengths of major neurites. At 2 DIV, the average length of major neurites in group 2 was about 190  $\mu\text{m}$  (large-concave substrate:  $189.1 \pm 8.1 \mu\text{m}$ ; nanoporous substrate:  $192.5 \pm 8.6 \mu\text{m}$ ), which was about twice as long as major neurites from group 1 (flat substrate:  $103.8 \pm 5.5 \mu\text{m}$ ; small-concave substrate:  $110.2 \pm 5.4 \mu\text{m}$ ). Overall, major neurites stretched out earlier from the soma and grew more vigorously on the large-concave and nanoporous substrates (group 2). These results indicated that neurons responded mostly to the pitch of nanotopographies, as there was no significant difference between the results from large-concave substrates and nanoporous substrates. The depth of the pore, which was the only difference between the large-concave and nanoporous substrates, was not a contributing factor to the observed effect.

Our results suggest that nanostructures with a pitch of 400 nm had an accelerating effect on neuronal polarization or axon formation, which is represented by the large portion of stage 3 neurons and longer neurites. Structures with a longer pitch in combination with adhesive molecules may have served as external cues to enhance the initiation of neuronal polarity. FE-SEM images imply possible different interactions between neurites and the AAO structures (Figure 4). On the



**Figure 4.** Morphological features of neurite outgrowth on topographically different substrates (2 DIV): a) small-concave substrate, b,c) large-concave substrate, and d) nanoporous substrate. Scale bars: 500 nm. Arrow indicates a needlelike point formed by AAO nanostructures.

small-concave substrates, neurites made continuous contact with the surface, and the scale of the AAO structures seemed to be relatively small in comparison with the size of neurites. On the other hand, neurites grown on group 2 substrates made intermittent or “jumping” contact with the surface through the peaks (tips or ridges) of the structures. In these cases, the FE-SEM images (Figure 4 b–d) strongly suggest that the nanoscale peaks were the major interaction spots between cell membranes (or growth cones) and the surfaces. On these spots, mechanical stimulations by the peaks could recruit new adhesion molecules and trigger intracellular signaling pathways (e.g. glycogen synthase kinase3 $\beta$ , PAR

proteins, Rho GTPases) implicated in the regulation of cytoskeleton dynamics and axon formation. Therefore, a lower density of interactions or sensing environments provided by the longer-pitched structures to growth cones may have led to the accelerated neurite outgrowth.

In summary, we identified pitch-dependent acceleration of neurite outgrowth by culturing primary hippocampal neurons on four different AAO-based topographical environments, which were classified as flat, small-concave, large-concave, and nanoporous substrates. We especially focused on the first two days during culture, since the nanotopographical effect is mainly expressed during the early period of cell culture. Interestingly, neurite development was found to be much faster on surfaces with a 400 nm pitch than on surfaces with a 60 nm pitch. This study implies that nanostructures with a particular surface topography can be a useful tool for the control of neurite development. We also believe that the control of the growth and development of nerve cells by nanotopography could open new opportunities in neurochemistry and bioengineering, such as novel scaffold design for neurons.

### Experimental Section

**Surface modification of substrates:** A 1% (v/v) solution of *N*-(2-aminoethyl)3-aminopropyltrimethoxysilane in a mixture of methanol and water (95:5) was acidified to pH 5.0 with acetic acid. The AAO substrates, including coverslips, were oxidized by an oxygen plasma cleaner (Harrick PDC-002, medium setting) for 20 min to maximize the surface density of OH groups. The oxidized substrates were immersed in the solution of the silane. After 2 h, the substrates were washed thoroughly with methanol and water, dried under a stream of argon, and baked in an oven at 110°C for 15 min.

**Cell culture:** Primary hippocampal neurons were cultured under serum-free conditions. Dissected E18 rat hippocampus tissue was incubated with 0.25% trypsin for 15 min at 37°C, and residual trypsin was rinsed off with the Hank balanced salt solution (HBSS). The digested hippocampus was triturated in HBSS (1 mL) with a fire-polished Pasteur pipette. The cell suspension was centrifuged for 3 min at 1000 rpm, and the resulting cell pellet was extracted. The pellet was suspended again in Neurobasal Medium supplemented with B27, L-glutamine (2 mM), L-glutamic acid (12.5  $\mu\text{M}$ ), and penicillin–streptomycin by using a Pasteur pipette. Dissociated cells were seeded at a density of 50 cells/ $\text{mm}^2$  on the prepared substrates. Cultures were maintained in an incubator (5%  $\text{CO}_2$ , 37°C). Half of the medium was replaced with fresh culture medium without L-glutamic acid every 3–4 days. All animal procedures were carried out in accordance with animal-use protocols approved by KAIST Institutional Animal Care and Use Committee (IACUC).

**Live/dead staining:** Ethidium homodimer 1 (10  $\mu\text{L}$ ) and calcein acetoxyethyl ester (2.5  $\mu\text{L}$ ) were mixed in phosphate-buffered saline (5 mL) in a 15 mL conical tube, which was then covered with aluminum foil to prevent fluorescence bleaching. The cell medium was removed from all cultures by a suction method. PBS (1 mL) and the prepared dye solution (200  $\mu\text{L}$ ) were added sequentially to each cell culture. The samples were covered with aluminum foil and placed in an incubator (5%  $\text{CO}_2$ , 37°C). After 20 min, the samples were taken out, the solution was removed from all cultures, and PBS (1 mL) was added to each cell culture.

Received: June 1, 2010

Revised: August 31, 2010

Published online: September 30, 2010

**Keywords:** anodized aluminum oxide · cell adhesion · nanostructures · neurite outgrowth · neurochemistry

- [1] M. Tessier-Lavigne, C. S. Goodman, *Science* **1996**, 274, 1123.
- [2] S. Mitragotri, J. Lahann, *Nat. Mater.* **2009**, 8, 15.
- [3] a) A. V. Sapelkin, S. C. Bayliss, B. Unal, A. Charalambou, *Biomaterials* **2006**, 27, 842; b) Y. W. Fan, F. Z. Cui, S. P. Hou, Q. Y. Xu, L. N. Chen, I.-S. Lee, *J. Neurosci. Methods* **2002**, 120, 17.
- [4] L. A. Cyster, K. G. Parker, T. L. Parker, D. M. Grant, *Biomaterials* **2004**, 25, 97.
- [5] a) T. Gabay, E. Jakobs, E. Ben-Jacob, Y. Hanein, *Physica A* **2005**, 350, 611; b) M. K. Gheith, V. A. Sinani, J. P. Wicksted, R. L. Matts, N. A. Kotov, *Adv. Mater.* **2005**, 17, 2663.
- [6] J. M. Bruder, A. P. Lee, D. Hoffman-Kim, *J. Biomater. Sci. Polym. Ed.* **2007**, 18, 967.
- [7] J. N. Hanson, M. J. Motala, M. L. Heien, M. Gillette, J. Sweedler, R. G. Nuzzo, *Lab Chip* **2009**, 9, 122.
- [8] N. M. Dowell-Mesfin, M.-A. Abdul-Karim, A. M. P. Turner, S. Schanz, H. G. Craighead, B. Roysam, J. N. Turner, W. Shain, *J. Neural Eng.* **2004**, 1, 78.
- [9] W. Hällström, T. Martensson, C. Prinz, P. Gustavsson, L. Montelius, L. Samuelson, M. Kanje, *Nano Lett.* **2007**, 7, 2960.
- [10] a) J. Xie, M. R. MacEwan, X. Li, S. E. Sakiyama-Elbert, Y. Xia, *ACS Nano* **2009**, 3, 1151; b) A. F. Quigley, J. M. Razal, B. C. Thompson, S. E. Moulton, M. Kita, E. L. Kennedy, G. M. Clark, G. G. Wallace, R. M. I. Kapsa, *Adv. Mater.* **2009**, 21, 1; c) J. M. Corey, D. Y. Lin, K. B. Mycek, Q. Chen, S. Samuel, E. L. Feldman, D. C. Martin, *J. Biomed. Mater. Res. Part A* **2007**, 83, 636.
- [11] A. Shalek, J. T. Robinson, E. S. Karp, J. S. Lee, D.-R. Ahn, M.-H. Yoon, A. Sutton, M. Jorgolli, R. S. Gertner, T. S. Gujral, G. MacBeath, E. G. Yang, H. Park, *Proc. Natl. Acad. Sci. USA* **2010**, 107, 1870.
- [12] a) A. M. Rajnicek, S. Britland, C. D. McCaig, *J. Cell Sci.* **1997**, 110, 2905; b) A. M. Rajnicek, C. D. McCaig, *J. Cell Sci.* **1997**, 110, 2915.
- [13] N. Gomez, S. Chen, C. E. Schmidt, *J. R. Soc. Interface* **2007**, 4, 223.
- [14] a) S.-K. Hwang, S.-H. Jeong, H.-Y. Hwang, O.-J. Lee, K.-H. Lee, *Korean J. Chem. Eng.* **2002**, 19, 467; b) O. Jessensky, F. Müller, U. Gösele, *Appl. Phys. Lett.* **1998**, 72, 1173; c) A. P. Li, F. Müller, A. Birner, K. Nielsch, U. Gösele, *J. Appl. Phys.* **1998**, 84, 6024.
- [15] W. K. Cho, S. Park, S. Jon, I. S. Choi, *Nanotechnology* **2007**, 18, 395602.
- [16] W. K. Cho, I. S. Choi, *Adv. Funct. Mater.* **2008**, 18, 1089.
- [17] M. Karlsson, E. Pålsgård, P. R. Wilshaw, L. D. Silvio, *Biomaterials* **2003**, 24, 3039.
- [18] B. Wolfrum, Y. Mourzina, F. Sommerhage, A. Offenhäusser, *Nano Lett.* **2006**, 6, 453.
- [19] S. Prasad, J. Quijano, *Biosens. Bioelectron.* **2006**, 21, 1219.
- [20] a) D. Kleinfeld, K. H. Kahler, P. E. Hockberger, *J. Neurosci.* **1988**, 8, 4098; b) J. Zheng, W.-H. Shen, T.-J. Lu, Y. Zhou, Q. Chen, Z. Wang, T. Xiang, Y.-C. Zhu, C. Zhang, S. Duan, Z.-Q. Xiong, *J. Biol. Chem.* **2008**, 283, 13280.
- [21] a) G. Banker, K. Goslin, *Culturing Nerve Cells*, The MIT Press, Cambridge, **1998**, p. 357; b) S. Kaeck, G. Banker, *Nat. Protoc.* **2006**, 1, 2406.